Syngas production by chemical-looping gasification of waste activated carbon with iron-based oxygen carrier

Xiao Li
Qingdao University of Science and Technology
An Mei
Qingdao University of Science and Technology
Man Wu
Qingdao University of Science and Technology
Jinshuai Li
Qingdao University of Science and Technology
Xiuli Zhang
Qingdao University of Science and Technology
Jilai Wu
Qingdao University of Science and Technology
Sijie Yuan
Qingdao University of Science and Technology
Qingjie Guo (ajeedit01@126.com)

Research

Keywords: chemical looping gasification, cyclic properties, iron-based oxygen carrier, synthesis gas, waste activated carbon

Posted Date: May 23rd, 2020

DOI: https://doi.org/10.21203/rs.3.rs-29625/v1

Syngas production by chemical-looping gasification of waste activated carbon with iron-based oxygen carrier

Xiao Li[a], An Mei [b], Man Wu[a], Jinshuai Li[a], Xiuli Zhang[a], Jilai Wu[a], Sijie Yuan[a], Qingjie Guo[a,b*]

[a]*Key Laboratory of Clean Chemical Processing of Shandong Province, College of Chemical Engineering, Qingdao University of Science and Technology, Qingdao 266042, PR China*

[b] *State Key Laboratory of High-efficiency Coal Utilization and Green Chemical Engineering, College of Chemistry and Chemical Engineering, Ningxia University, Yinchuan 750021, PR China*

Abstract Waste activated carbon (WAC), as a typical solid waste, can be utilized by chemical looping gasification (CLG) technology with an iron-based oxygen carrier to produce valuable synthesis gas. A series of experiments on WAC of the CLG process have been carried out in a fixed-bed reactor. The operation parameters involving the OC/WAC mole ratio, steam flow rate and reaction temperature during CLG reactions have been investigated in detail. Further, the cyclic performance within 10 cycles has been also discussed. Fresh and cyclic reaction oxygen carrier samples have been analyzed by X-ray diffraction (XRD) and scanning electron microscopy (SEM). In order to obtain high-quality syngas with high carbon conversion, the optimal of OC/WAC mole ratio, steam flow rate and reaction temperature are 0.15, 0.10 mL/min,

Received: ; Revised: ; Accepted:

*Corresponding author: Tel: +86-0951-2061351; E-mail: qj_guo@yahoo.com (Q. Guo)

and 950 °C, respectively. The iron-based oxygen carrier exhibits a stable cyclic performance during the multiple tests, following the reaction path of $Fe_2O_3 \rightarrow Fe_{0.98}O$ in the individual reduction process. Moreover, the iron-based oxygen carrier could be oxidized almost to its initial state after 10 redox tests. No obvious sintering and agglomeration phenomena are observed. The WAC of CLG presents a new approach for the comprehensive utilization and disposal of solid waste, especially with low volatile feedstock.

Keywords: chemical looping gasification, cyclic properties, iron-based oxygen carrier, synthesis gas, waste activated carbon

1Introduction

As the best versatile absorbent, activated carbon (AC) is extensively used in various industrial processes for decades (Leong et al. 2018; Gamal et al. 2018). Because of the serious pore blockage, some of the spent activated carbon is difficult to regenerate and reutilize. Thus, it is usually discarded as solid waste from factories. Furthermore, these discarded waste activated carbons (WACs) are commonly disposed for landfills and via open burning treatment, which practices jeopardize the land security and threaten the air safety (Wong et al. 2018). Recognizing the aforementioned issues and considering the various disposal methods, the chemical looping gasification (CLG) technologies have attracted attentions due to their ability to convert carbonaceous waste to valuable products (Arnold and Hill 2019, Wang et al. 2019). Typically, WAC has the advantages of high carbon content. Hence, the WAC is a good candidate as a feedstock in the gasification processes.

The CLG could convert carbon-containing feedstock into value-added gas products in an oxygen-controlled atmosphere. Therefore, it is associated with the inherent separation of CO_2 (Lyngfelt 2014). Indeed, CLG is achieved with metal

oxides (Me_xO_y) called oxygen carriers (OCs), which are employed as oxygen sources. The oxygen carrier is continuously transported and circulated between two interconnected chambers. The oxygen required for gasification is provided by lattice oxygen released from the OC, which lead to the lower cost without air separation. Moreover, the lattice oxygen is capable of avoiding combustion reactions by controlling the mole ratio between fuels and OCs. The schematic diagram of CLG process for synthesis gas production is exhibited in Fig. 1.

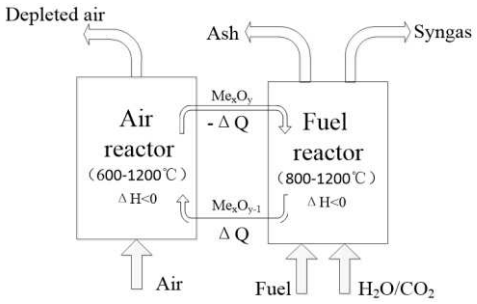

Fig. 1 Schematic of a fixed bed reactor.

The OC is the crucial backbone in the chemical looping process. Recently, a large number of oxygen carriers have been reported in CLG processes, such as Fe (Huang et al. 2016), Ni (Medrano et al. 2015), and Mn (Yin et al. 2018). The iron-based OC is the most common option, due to the inexpensive, durable, stable, moderately reactive, nonpoisonous, and resistant to sintering or attrition (Zhao et al. 2017; Liu et al. 2018). Huseyin et al. (2014) tested biomass CLG using Fe_2O_3/Al_2O_3 as an oxygen carrier in a 10 kWth interconnected fluidized bed reactor. The OC performed good stability and reactivity during 60-h continuous runs. In particular, the Fe_2O_3/Al_2O_3 demonstrated excellent performance in the utilization of waste resources, such as sewage sludge, waste water and municipal solid waste (Chen et al. 2019). Huang et al. (2017) used natural hematite as an oxygen carrier in sewage sludge disposal. The results showed that the carbon conversion of fuel had increased by 36.29%. The hematite also exhibited good performance during continuous tests for 23 h. Qin et al. (2018) investigated Fe_2O_3/Al_2O_3 using the CLG process of organic waste water to produce high H_2/CO ratio syngas. The Fe_2O_3/Al_2O_3showed an otable

performance and achieved auto-thermal feasibility in this CLG process. The highest syngas yield of 3.325 L/g was obtained with almost 100 % carbon conversion.

The resource utilization of WAC to produce synthesis gas would be achieved by CLG with opening a broader means for treatment of carbonaceous solid wastes. The purpose of this work is to verify the feasibility of iron-based OCs for the treating of WAC in CLG, focusing on macroscopic research combining various analytical methods. A series of experiments were carried out to investigating the effect of parameters including the mole ratio between the OC and WAC, reaction temperature and steam flow on the gasification process. Afterward, the stability of the OC during multiple redox reactions was also discussed, and 10-cycle experiments were conducted. Finally, the fresh and used OC were collected and analyzed with X-ray diffraction (XRD) and scanning electron microscopy (SEM) to better reveal the crystalline phase transformation and surface morphology changes, respectively.

2 Materials and experimental

2.1 Materials

A typical waste activated carbon was collected from sugar factory in Shandong Province, China. The samples were dried at 90°C for 2h and then ground and sieved into an approximate size of 80~200 μm. The proximate and ultimate analyses, and lower heating values of the WAC are provided in Table 1.

Table 1 Proximate and ultimate analysis of WAC after pretreatment

Sample	Proximate analysis w_{ad} (%)				Ultimate analysis w_{ad} (%)					LHV(MJ/kg)
	A	M	V	FC	C	H	N	S	O[①]	
WAC	11.87	1.40	37.43	55.14	71.62	2.96	3.83	1.64	3.84	14.14

ad: air dried basis

①: Calculated by difference

2.2 Oxygen carrier preparation

The Fe_2O_3/Al_2O_3 oxygen carrier was prepared using the impregnation method. A given amount of $Fe(NO_3)_3.9H_2O$ was dissolved in deionized water for preparation of the saturated solution. Here, Al_2O_3 powder was added into the saturated solution as an inert support. Then, the mixture solution was stirred and heated at 80 °C until the water was evaporated. After that, the residue was dried at 120 °C for12 h. Then, it was transferred into a muffle furnace and calcined at 900°C for 3 h under an air atmosphere. Finally, the obtained precursors were crushed and sieved into ~100 μm.

2.3 Experimental procedure

To simplify the CLG reaction process of WACs, a series of experiments were implemented in a fixed-bed reactor to test the feasibility of WAC disposal using CLG. The schematic diagram is illustrated in Fig.2. The proposed apparatus are composed of a quartz tube reactor, a mass flow controller, a steam generator section, a cooling system, an exhaust gas sampling container, and an analysis system. The tube reactor was heated by an electronic furnace. The temperature was controlled by a thermocouple surrounding the tube. The steam generator was composed of a constant flow pump for steam generation through preheating by a furnace at 300°C.

In the reduction stage of each test, a mixture of WAC and oxygen carrier with various OC/WAC ratios (0, 0.1, 0.15, 0.2, and 0.25) was initially loaded in a quartz boat and placed on the cool zone of the tube. High-purity argon was used as the purge gas at 200 mL/min for 15 min in advance to remove the air. When the reactor reached the desired reaction temperature (750, 800, 850, 900, and 950 °C), argon was replaced by a mixture stream of different steam flow rates (0, 0.05, 0.10, 0.15, and 0.20 mL/min). Next, the argon was used to flush the gasification reactor for 5 min. After that, the quartz boat was rapidly moved into the heating zone, and the gasification time was 60 min, which was sufficient time for the reaction. The exit gas was passed through for cooling, purifying and drying. Finally, the generated gases were collected via a group of sampling bags at 5 min intervals. During the oxidation period, the

reduced OC was oxidized by air at a volumetric flow rate of 200 mL/min in a tubular furnace. The oxidation time was set to 60 min. Since the reaction system was a batch system, the OC particles were alternatively exposed to oxidation and reduction stages to simulate the circulating experiments. The compositions of the flue gas were measured by off-line gas chromatography with a TCD detector. After the reactor cooled to ambient temperature, the selected oxygen carrier particles were collected for characterization analysis.

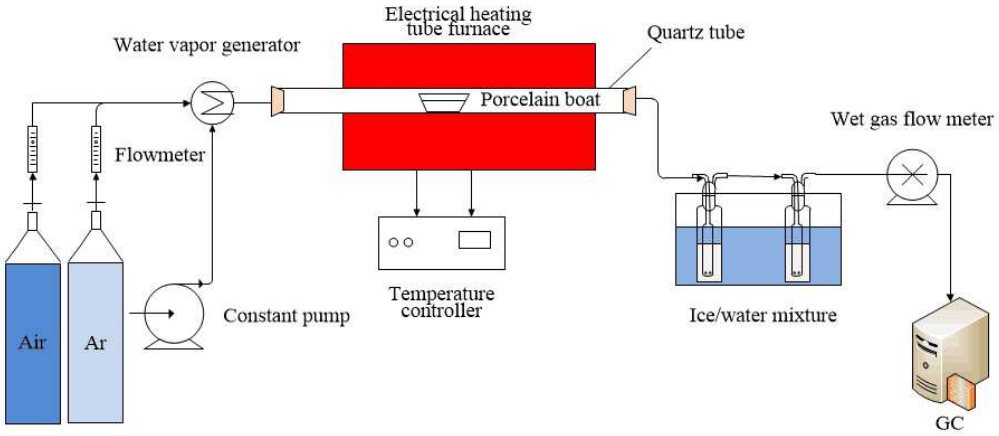

Fig. 2 Schematic of a fixed bed reactor

2.4 Oxygen carrier Characterization

To better understand the reaction mechanism, a series of characterization methods were employed. The crystalline phase of the oxygen carrier samples were confirmed with X-ray diffraction using Cu-Kα radiation with 40 kV and a current of 40 mA. The samples were scanned in the 2θ range of 5-80°with a step range of 0.02°. Moreover, scanning electron microscopy (SEM) using a Hitachi S4800 was used to evaluate the morphology surface features of the oxygen carrier samples at the different stages.

2.5 Data processing

(1) In each part, the relative gas content (C_i) of each component in the dry basis outlet gas can be evaluated as follows:

$$C_i=\frac{\int_0^t v\cdot y_i\, dt}{\int_0^t v\cdot y\, dt} \quad (1)$$

Where y_i represents the actual volume fraction of gas species i (H_2, CO, CH_4, and CO_2) in the dry outlet gas; v denotes the volume flow rate of the dry basis flue gas in the outlet.

(2) The lower heating value (LHV, MJ/Nm^3) of the generated gas products can be calculated as follows:

$$LHV= 126C_{CO}+108C_{H2}+388C_{CH4} \quad (2)$$

(3) The gas yield (G_v, Nm^3/kg) is the volume of dry basis gas product yielded from the unit mass of WAC sample, calculated as follows:

$$G_v =\frac{\int_0^t v\cdot(y_{CO}+y_{CO2}+y_{CH4}+y_{H2})dt}{M_{WAC}} \quad (3)$$

(4) The carbon conversion efficiency of the WAC (η_c,%) is the proportion of the carbon fraction of carbon-containing gas in the outlet gas to the carbon fraction of the WAC fed into reactor, where C_C% is the carbon content of the WAC:

$$\eta_c=\frac{12(C_{co}+C_{co_2}+C_{CH_4})\cdot G_v}{24.45\cdot Cc\%\cdot M_{WAC}} \quad (4)$$

(5) The effective gas content (Y_g, %) is defined as the ratio of the volume of effective gases (H_2, CO, CH_4) to the total amount of gas produced by WAC:

$$Y_g=\frac{\int_0^t(V_{CO}+V_{H_2}+V_{CH_4})dt}{\int_0^t(V_{CO}+V_{CO_2}+V_{CH_4}+V_{H_2})dt} \quad (5)$$

(6) The syngas yield (Nm^3/kg) is the addition of effective gas yield:

$$V_g=\frac{\int_0^t v\cdot(y_{CO}+y_{CO_2}+y_{CH_4})dt}{M_{WAC}} \quad (6)$$

3 Results and discussion

3.1 Effect of (OC/WAC) ratio

The OC was displayed as an oxygen source and heat carrier. A series of comparison experiments were conducted to obtain the optimal OC/WAC value. In addition, without active role, Al_2O_3 was used as the bed material for the blank experiment for comparison.

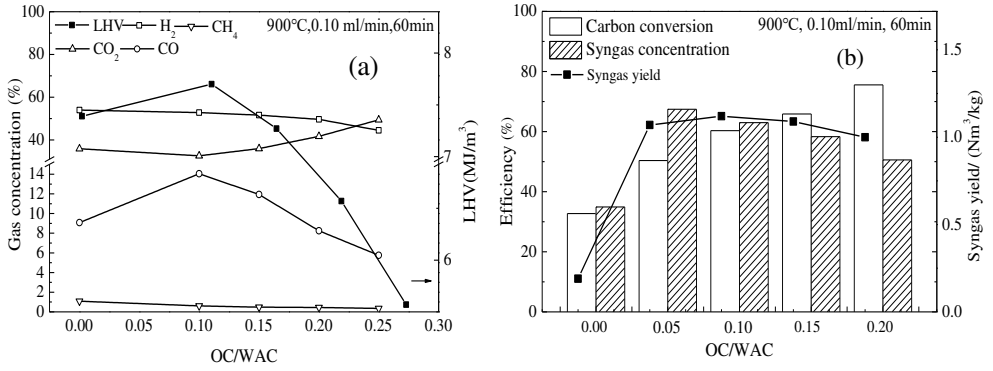

Fig. 3 Gasification characteristics of WAC with different OC/WAC

The effect of OC/WAC mole ratio on gas distribution and LHV are shown in Fig. 3a. H_2 is consumed at first, due to the low activation energy as shown in the reaction (7). Thus H_2 content gradually decreases with the increase of OC/WAC. Mainly ascribed to the supplement of suitable lattice oxygen put rightward the reaction (10), CO concentration firstly increases when OC/WAC is lower than 0.1. However, CO declines sharply while the CO_2 inclines monotonously as the OC/WAC increases from 0.10 to 0.25. This can be explained that excess lattice oxygen promoted the reactions shown in reaction (7) and (8). The combustible gases were consumed to more CO_2 and H_2O generation, indicating that gasification process gradually was replaced by combustion process in this case. CH_4 content declines slightly with an increasing OC/WAC, on account of the reaction (9). Meanwhile, LHV firstly increases at the OC/WAC range of 0 to 0.1, reaching its maximal of 7.70MJ/Nm^3. Then it abruptly decreases when OC/WAC is exceeded 0.10 with the minimum value of 5.66 MJ/Nm^3 at OC/WAC of 0.25. The results meant that extra OC would provide excess lattice oxygen, causing the consumption of large amount synthesis gas.

In order to further understand the effect of OC/WAC in the CLG process, the vital variables of carbon conversion, syngas concentration and syngas yield are shown

in Fig.3b. Due to the promoting the WAC conversion, carbon conversion gradually increases from 32.72% to 75.53% as the increasing of OC/WAC from 0 to 0.25. Meanwhile, the syngas concentration and syngas yield are up to 67.41% and 1.12 Nm^3/kg, respectively. It resulted that the syngas generation were evidently enhanced with the addition of OC. Because the OC was prone to achieve the partial oxidize the WAC with producing the target gaseous products (Wei et al. 2019). Besides, the OC enhanced the water-gas shift reaction to generate more H_2 (Deng et al. 2019). However, when the OC/WAC was more than 0.1, syngas concentration and syngas yield drastically decreased. This mainly attributed to a part of combustible gas was completely oxidized by the excess lattice oxygen of OC, which was adverse to syngas generation. In general, the higher OC/WAC meant the more OC added in reactor, which significantly promoted WAC conversion but sacrificed synthesis gas yield. Aiming at the target of high-efficiency resource utilization of WAC, the OC/WAC ratio was determined at 0.15, where the highest LHV value of 7.67MJ/Nm^3 was obtained. The reactions associated with OC are listed as followed:

$$H_2 + 1.042Fe_2O_3 = 2.127Fe_{0.98}O + H_2O \quad \triangle H_{1173K} > 0 \quad \triangle G_{1173K} < 0 \tag{7}$$

$$CO + 1.042Fe_2O_3 = 2.127Fe_{0.98}O + CO_2 \triangle H_{1173K} < 0 \triangle G_{1173K} < 0 \tag{8}$$

$$CH_4 + 4.17\ Fe_2O_3 = 8.511Fe_{0.98}O + CO_2 + 2H_2O \quad \triangle H_{1173K} > 0 \triangle G_{1173K} < 0 \tag{9}$$

$$C + 1.042Fe_2O_3 = 2.127Fe_{0.98}O + CO \quad \triangle H_{1173K} > 0 \triangle G_{1173K} < 0 \tag{10}$$

3.2Effect of steam flow rate

Considering the target of further enhancing the WAC conversion and synthesis gas yield, especially the H_2 yield, steam was employed as a gasifying agent during the

CLG of WACs.

The flue gas concentration and LHV variation under different steam flow rates are shown in Fig.4a. In the absence of steam, the H_2 concentration and LHV are the lowest at 17.69% and 4.18 MJ/Nm^3, but CO_2 is the highest at 65.07%. With the increase in steam flow rate, the H_2 concentration shows an evident uptrend. Whereas, the concentration of CO decreases overall. The CH_4 concentration remains nearly invariable. Based on evaluations of the synthesis gas concentration, the LHV increases substantially from 4.18 MJ/Nm^3 to 6.95 MJ/Nm^3 as the steam flow rate reaches 0.05 mL/min, while the LHV increases mildly when the flow rate is higher than 0.10 mL/min.

Owing to the addition of H_2O, the H_2 generation and CO consumption were facilitated with the water-gas shift reaction (12) shifting toward the right. It was noteworthy that the CO content presented a fluctuation trend, possibly because of the competition effects between reactions (11), (12) and (13). Because the fixed carbon of WACs preferentially reacted with steam to generate CO rather than undergoing solid-solid reactions between OC and WAC particles. The CO_2 concentration decreased overall, and it was much lower than that of without steam. This result suggested that an appropriate steam addition significantly improves the syngas yield, especially H_2 generation, which contributed to enhance the quality of synthesis gas.

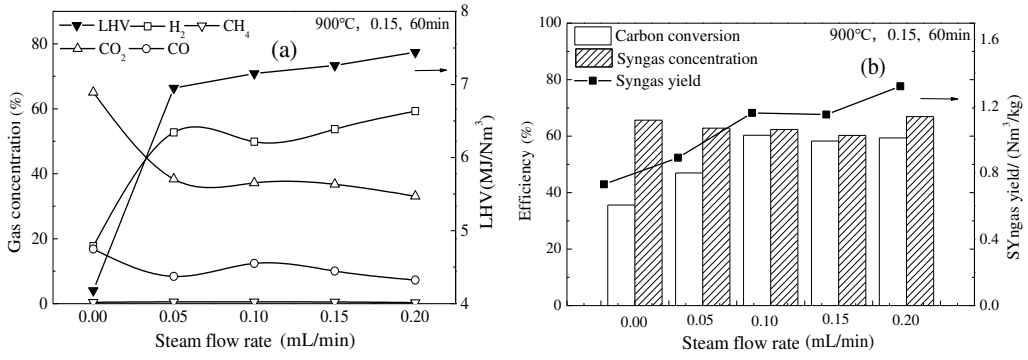

Fig.4 Gasification characteristics of WAC with different steam flow rate

$C+CO_2 = 2CO$ $\triangle H_{1173K} = +168.84kJ/mol$ (11)

$C+H_2O= CO + H_2$ $\triangle H_{1173K} = +135.71kJ/mol$ (12)

$C+2H_2O = CO_2+H_2$ $\triangle H_{1173K} = +141.3kJ/mol$ (13)

$CO+H_2O= CO_2+H_2$ $\triangle H_{1173K} = - 41.18$ kJ/mol (14)

Additionally, the effect of steam flow rate on carbon conversion, syngas concentration and syngas yield is displayed in Fig.4b. Carbon conversion presents an increasing tendency and then decreases slightly as the increasing of steam flow rate with the maximum value of 60.3% at 0.10 mL/min. The syngas concentration first decreases and then gradually increases to 66.9% at 0.20 mL/min. The syngas yield presents an overall uptrend with the first growing rapidly and then moderates. This may have resulted from the reduction reactions being close to chemical equilibrium. On the one hand, the steam could evidently promoted carbon conversion and improved the contact between solid reactants as an oxygen source. Accordingly, solid-solid reactions between the OC and WAC were improved (Huang et al. 2016). On the other hand, the more steam facilitated the water-gas shift reaction to the right to generate more H_2. Generally, the steam actually accelerated the syngas yield, especially H_2 yield. However, it was notable that the excessive steam (>0.10 mL/min) had no apparent impact on carbon conversion. At the same time, the more steam would shorten the residence time between the gas phase and solid phase. The reactions between the WAC and steam were particularly inhibited. Thus, the WAC conversion and gas yield were restricted within high steam amounts. The flow rate of 0.10 mL/min was selected as the proper steam flow rate, where the carbon conversion of 60.3% and LHV of 7.15 MJ/Nm^3were achieved.

3.3 Effect of reaction temperature

Reaction temperature was a key parameter for the fuel conversion and OC performance in the CLG processing (Taba et al. 2012). In this study, a series of experiments corresponding to the effect of gasification temperature on WAC in the CLG were implemented.

Fig. 5 depicts the gas distribution and LHV as functions of reactor temperature. The high temperature can drastically improve the WAC conversion and syngas yield. The concentrations of H_2 and CO increase with the increasing of temperature, while CO_2 presents the opposite trend. The concentration of CH_4 remains almost constant. According to the increase in combustible gas concentrations, the LHV increases rapidly from 3.72 MJ/m^3 at 750 °C to 7.39 MJ/m^3 at 950 °C. Furthermore, the effects of temperature on carbon conversion and syngas concentration are shown in Fig. 5b. As a result, the syngas concentration presents a monotonically increasing trend with the ramping up of temperature. The carbon conversion increases drastically from 26.59% to 71.54% as the temperature increased from 750 °C to 950 °C. Meanwhile, the syngas yield attains the maximum values of 1.47 Nm^3/kg at 950 °C. Accordingly, the high temperature was conducive for WAC thermal conversion and syngas yield.

The elevated temperatures favored the endothermic reactions (11), (12) and (13), which generated the more combustible gases. In addition, the endothermic reaction (14) was inhibited by a high temperature, which led to the decreasing of CO_2. This indicated that high temperatures were favorable for generating syngas with high calorific values. In addition, the OC presented poor reactivity under low temperatures, leading to the limited of carbon conversion and syngas products. Accompany the temperature rising, the more lattice oxygen was released. So the WAC conversion was enhanced. Generally, a high reaction temperature was necessary for WAC thermal conversion and high-quality synthesis gas yields. Thus, 950 °C was the optimum reaction temperature for the CLG process of WAC. At this temperature, the carbon conversion, syngas yield, and LHV attained maximum values were 71.54%, 1.47 Nm^3/kg, and 7.39 MJ/Nm^3, respectively.

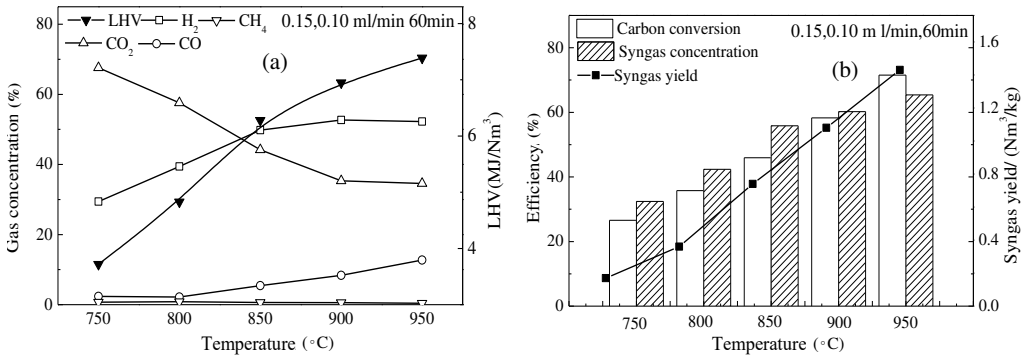

Fig. 5 Gasification characteristics of WAC under different temperature

3.4 Effect of numbers of cycles

In order to evaluate the reactivity stabilization of OCs in the CLG process, the multi-cycle tests were carried out in a fixed-bed reactor. The reaction temperature, OC/WAC, steam flow rate, and reaction time were fixed at 900°C, 0.15, 0.10 mL/min and 60 min, respectively.

As illustrated in Fig. 6, the concentration of CO_2 shows a slight downward trend with the increasing of cycle numbers. While the CO concentration presents a slight upward trend. The concentration of H_2 also increases at the range from 49.50 % to 53.21 % over the cycles. There is no remarkable change in CH_4 content. The value of LHV increases from 7.09 MJ/Nm^3 in the 1st redox cycle to 7.75 MJ/Nm^3 in the 10th cycle. The carbon conversion shows a downward trend from 58.95% to 53.11% during the tests. The syngas concentration gradually increases and reaches the maximum value of 65.28% in the 10th cycle. Meanwhile, the syngas yield slightly decreases but remains above 1.03 Nm^3/kg. Although, the OC reactivity shows a slight deactivation trend after 10 cycles, especially when the oxidation ability of the OC tends to be moderate, leading to a slight decreasing of CO_2 concentration and an elevated calorific value of gases. The Fe_2O_3/Al_2O_3 still presented a favorable cycle performance in a comparatively long run of cycles for the CLG of WAC.

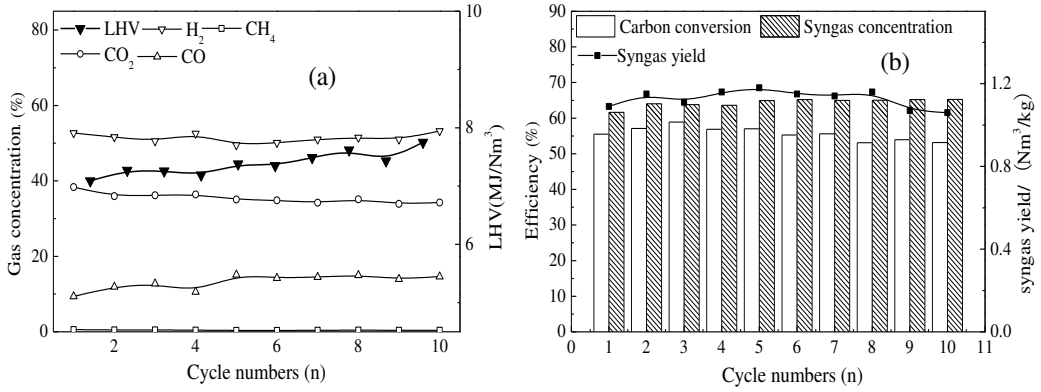

Fig.6 Gasification characteristics of WAC under different temperature

3.5 Characterization of OCs

To further understand the reactivity variation of OCs during the CLG test, the crystalline phase transformation and surface morphology of the OCs were characterized by XRD and SEM. The fresh OC and the OC samples after the 1st reduction and the 10th redox cycle were collected for analysis.

The XRD patterns of the OC samples in different stages are shown in Fig. 7. The fresh OC mainly consists of Fe_2O_3 and Al_2O_3. The Fe_2O_3 is the active component and oxygen carrier to release lattice oxygen. While, the Al_2O_3 is the inert carrier. After the 1st reduction process of the OC in the CLG process, the crystalline phases of $Fe_{0.98}O$ and Al_2O_3 are detected. This indicated that $Fe_{0.98}O$ was the predominant crystal formed from the active component after the individual reduction. Meanwhile, little change could be observed in the inert Al_2O_3 phase. In the 10th cycle sample, the results of main diffraction peak show that Fe_2O_3 (PDF: 33-0664) still is the main active constituents and Al_2O_3 is the inert constituent.

The active oxygen carrier component Fe_2O_3 was reduced to $Fe_{0.98}O$ after CLG of the WAC. The reduction process of Fe_2O_3/Al_2O_3 followed the path $Fe_2O_3 \rightarrow Fe_{0.98}O$. Negative changes to the particles including through sintering and agglomeration usually occurred during the phase transition from FeO to Fe (Adanez et al. 2012).

Although it had no ability to release lattice oxygen and directly reacted with the WAC at high temperature. The unreacted fuel and WAC ash covered the OC surface, which was responsible for the reduction of the Al_2O_3 phase. The iron-based OC was almost regenerated to its original state over the oxidation stage after multi-redox cycles. Therefore, the XRD results indicated that the iron-based oxygen carrier had a favorable cycle performance in the CLG process.

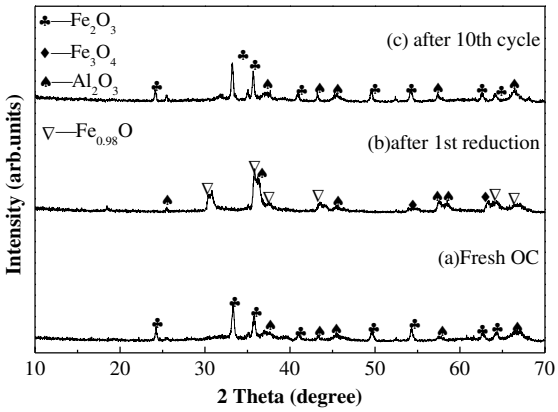

Fig.7XRD patterns of fresh and used OC samples

Scanning electron microscopy (SEM) was used to evaluate the morphology of OC samples. As illustrated in Fig. 8a, the surface structure of the fresh sample is tough and loose with a porous structure. It was beneficial for the diffusion and reactions of reactants (Das et al. 2018). After the 1st cycle, the greater porosity structure was observed than that of fresh sample. It was ascribed to gas escaping from the interior of OC particles (Deng et al. 2019). In this case, the structure was conducive for the penetration of gaseous reactants into the core of the OC particles. Therefore, the performance of OC was increased in the former cycles. Finally, as shown in Fig. 8c, agglomeration is observed in the 10th sample. Some small granules merge into larger granules. It was adverse to the reaction between the OC and other reactants. This may have resulted from the lattice transfer and continuous thermal stress at high temperatures during the multiple tests. Some WAC ash might block the pore and cause a negative change to the surface structure as well. However, it still

remained porous. These results indicated that iron-based oxygen carriers were a promising candidate in the WAC CLG process.

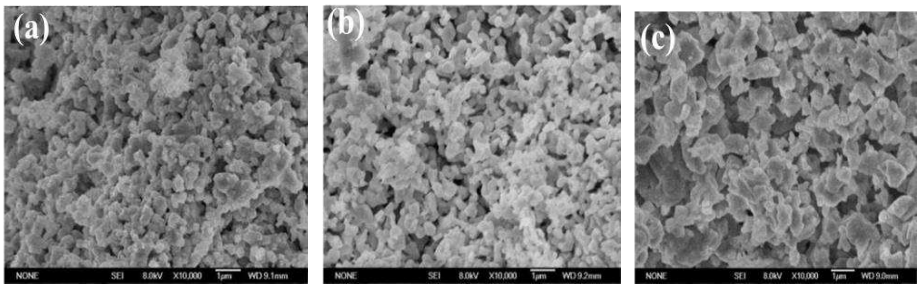

(a) Fresh sample (b) 1st sample (c) 10th sample

Fig. 8 SEM images of Fresh and used OC samples

4. Conclusions

This work focused on verifying the feasibility of WAC in the CLG process using an iron-based oxygen carrier to produce a syngas product. The iron-based oxygen carrier showed favorable reactivity for syngas generation and WAC conversion. The effects of operation parameters were examined on a bench-scale fixed-bed reactor. The following conclusions are drawn based upon the results:

(1) The optimal OC/WAC mole ratio is determined at 0.15, where the highest yield of syngas product of 1.12Nm^3/kg and the acceptable carbon conversion of 60.31% are obtained based on the trade off between WAC conversion and syngas yield.

(2) An adequate amount of steam introduction would promote WAC conversion and hydrogen generation. The relatively high carbon conversion of 60.31% and the LHV of 6.95 MJ/Nm^3 are reached at the steam flow rate of 0.10 mL/min .

(3) When the reaction temperature is 950 °C, the carbon conversion, syngas yield and LHV are maximized.

(4) The cyclic performances of the OC during 10-time cycle tests are evaluated.

Over the long run, no obvious change occurs in the crystalline phase and morphology structure based on the XRD and SEM results. The iron-based oxygen carrier exhibits good cycling performance.

(5) The oxygen carrier follows the reaction path of $Fe_2O_3 \rightarrow Fe_{0.98}O$ in the individual reduction process. Then it could be oxidized to its initial state after 10 redox cycle tests. In general, the comprehensive disposal of WAC by the CLG process with the iron-based oxygen provides a highly efficient and environmentally friendly way.

Acknowledgments

This work is funded by the Key Research and Development Program Project，the Ningxia Hui Autonomous region (2018BCE01002); The National Natural Science Foundation of China (201868025); The National Key Research and Development Program Project (2018YFB0605401); The National First-rate Discipline Construction Project of Ningxia (NXYLXK2017A04); The Key Research and Development Program Ningxia (2018BEE03009).

Nomenclature

AC	Activated carbon
WAC	Waste activated carbon
CLC	Chemical looping combustion
CLG	Chemical looping gasification
Me_xO_y	Metal oxide
OC	Oxygen carrier
CLR	Chemical looping reforming

A	Ash (wt%)
M	Moisture (wt%)
V	Volatile (wt%)
FC	Fixed carbon (wt%)
TCD	Temperature controlled detector
M	The mass of WAC (g)
LHV	Lower heat value
XRD	X-ray diffraction
SEM	Scanning electron microscopy
WGS	Water gas shift

References

Adanez J, Abad A, Garcia-Labiano F, Gayan P, Diego L F D (2012) Progress in chemical-looping combustion and reforming technologies. Progress in Energy & Combustion Science 38(2): 215-282.

Arnold RA, Hill JM (2019) Catalysts for gasification: a review. Sustainable Energy & Fuels 181(3): 656-672.

Chen P, Sun X, Gao M, Ma J, Guo Q (2019) Transformation and migration of cadmium during chemical-looping combustion/gasification of municipal solid waste. Chemical Engineering Journal 365: 389-399.

Das S, Deen NG, Kuipers HAM (2018) Multi-scale modeling of fixed-bed reactors with porous (open-cell foam) non-spherical particles: Hydrodynamics. Chemical Engineering Journal 334: 741-759.

Deng Z, Huang Z, He F, Zheng A, Wei G, Meng J, Zhao Z, Li H (2019) Evaluation of calcined copper slag as an oxygen carrier for chemical looping gasification of

sewage sludge. International Journal of Hydrogen Energy 44(33): 17823-17834.

Gamal ME, Mousa HA, El-Naas MH, Zacharia R, Judd S (2018) Bio-regeneration of activated carbon: a comprehensive review. Separation and Purification Technology 197: 345-359.

Huang Z, Xu G, Deng Z, Zhao K, He F, Chen D, Wei G, Zheng A, Zhao Z, Li H (2017) Investigation on Gasification Performance of Sewage Sludge Using Chemical Looping Gasification with Iron Ore Oxygen Carrier. International Journal of Hydrogen Energy 42(40): 25474-25491.

Huang Z, Zhang Y, Fu J, Yu L, Chen M, Liu S, He F, Chen D, Wei G, Zhao K, Zheng A, Zhao Z, Li H (2016) Chemical looping gasification of biomass char using iron ore as an oxygen carrier. International Journal of Hydrogen Energy 41(40): 17871-17883.

Huseyin S, Wei G, Li H, He F, Huang Z (2014) Chemical-looping gasification of biomass in a 10 kWth interconnected fluidized bed reactor using Fe_2O_3/Al_2O_3oxygen carrier. Journal of Fuel Chemistry and Technology 42(8): 922-931.

Leong KY, Loo SL, Bashir MJK, Oh WD, Rao PV, Lim J (2018) Bio-regeneration of spent activated carbon: Review of key factors and recent mathematical models of kinetics. Chinese Journal of Chemical Engineering 23(5): 893-902.

Liu GC, Liao YF, Wu Y, Ma X (2018) Application of calcium ferrites as oxygen carriers for microalgae chemical looping gasification. Energy Conversion & Management (160): 262-272.

Lyngfelt A. (2014) Chemical-looping combustion of solid fuels, Status of development. Applied Energy 113(1):1869-1873.

Medrano JA, Hamers HP, Williams G, Annal and MS, Gallucci F(2015) $NiO/CaAl_2O_4$ as active oxygen carrier for low temperature chemical looping applications. Applied Energy 158:86-96.

Qin W, Wang J, Luo L, Liu L, Xiao X, Zheng Z, Sun S, Hu X, Dong C (2018) Chemical looping reforming of ethanol-containing organic wastewater for high ratio H_2/CO syngas with iron-based oxygen carrier, International Journal of Hydrogen Energy 43(29): 12985-12998.

Shen T, Ge H, Shen L (2018) Characterization of combined Fe-Cu oxides as oxygen carrier in chemical looping gasification of biomass. International Journal of Greenhouse Gas Control75: 63-73.

Taba LE, Irfan MF, Wan Daud WAM, Chakrabarti MH (2012) The effect of temperature on various parameters in coal, biomass and CO-gasification: a review. Renewable and Sustainable Energy Reviews 16(8):5584-96.

Wang Y, Niu P, Zhao H (2019) Chemical looping gasification of coal using calcium ferrites as oxygen carrier. Fuel Processing Technology192: 75-86.

Wei G, Wang H, Zhao W, Huang Z, Yi Q, He F , Zhao K, Zheng A, Meng J, Deng Z, Chen J, Zhao Z , Li H (2019) Synthesis gas production from chemical looping gasification of lignite by using hematite as oxygen carrier. Energy Conversion and Management 185: 774-782.

Wong S, Ngadi N, Inuwa IM, Hassan O (2018) Recent advances in applications of activated carbon from biowaste for wastewater treatment: A short review, Journal of Cleaner Production 175: 361-375.

Yin S, Shen L, Dosta M, Hartge EU, Heinrich S, Lu P, Werther J, Song T (2018) Chemical looping gasification of biomass pellet with a Manganese ore as oxygen carrier in the fluidized bed. Energy & Fuels 32 (11): 11674-11682.

Zhao X, Zhou H, Sikarwar VS, Zhao M, Park AHA, Fennell PS, Shen L, Fan LS (2017) Biomass-based chemical looping technologies: the good, the bad and the future. Energy &Environmental Science, 10 (9): 1885-1910.

Figures

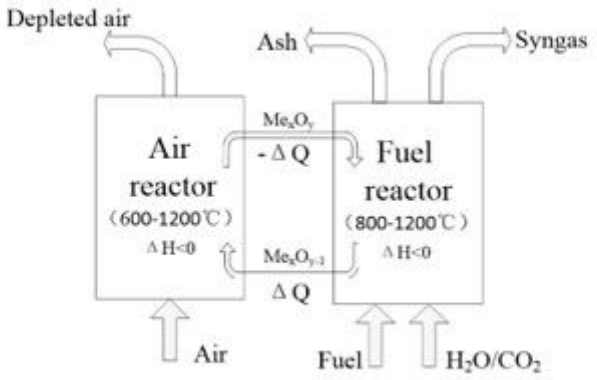

Figure 1

Schematic of a fixed bed reactor.

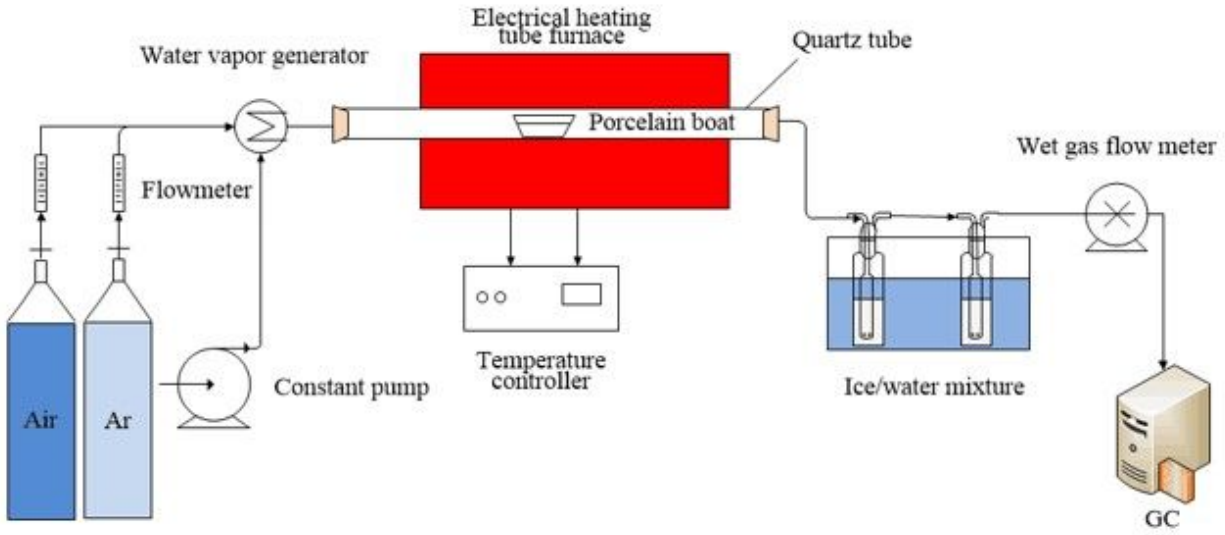

Figure 2

Schematic of a fixed bed reactor

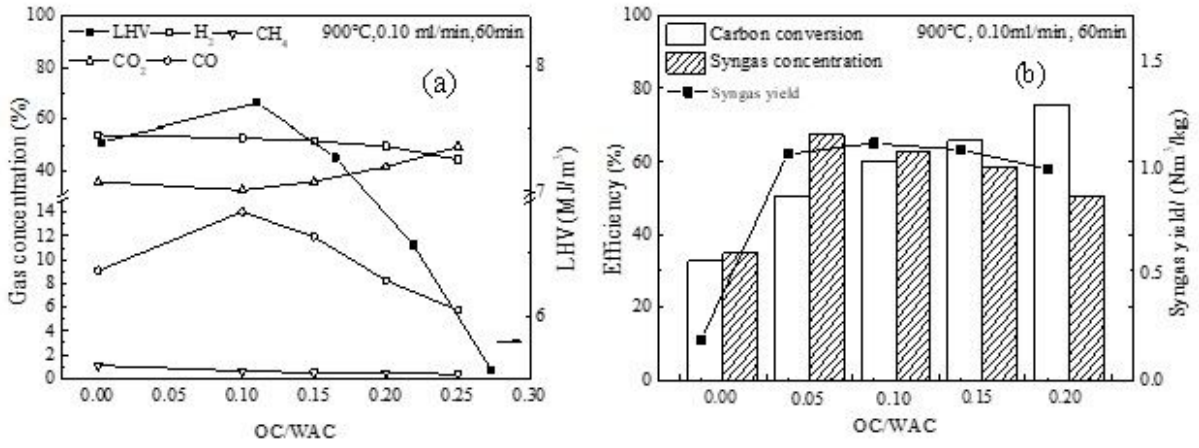

Figure 3

Gasification characteristics of WAC with different OC/WAC

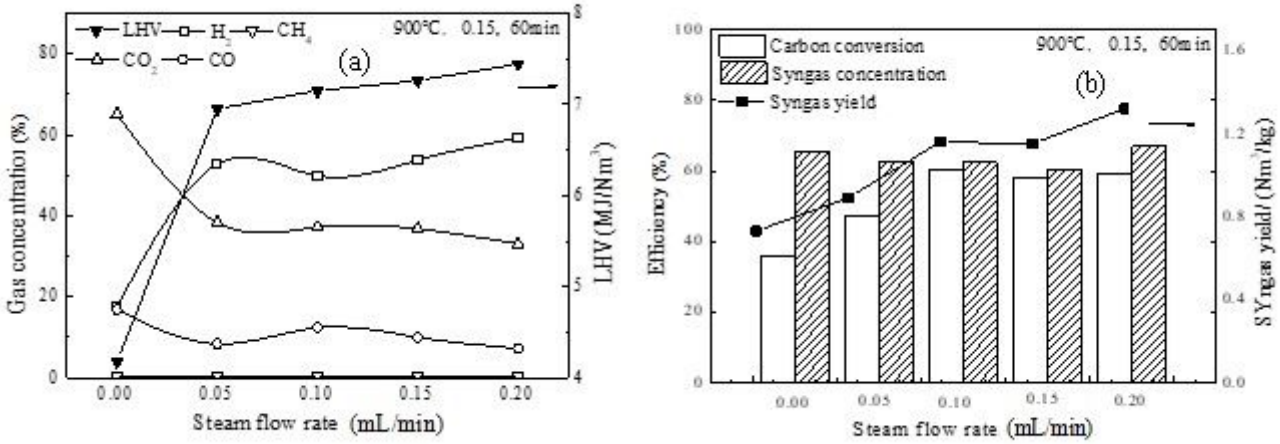

Figure 4

Gasification characteristics of WAC with different steam flow rate

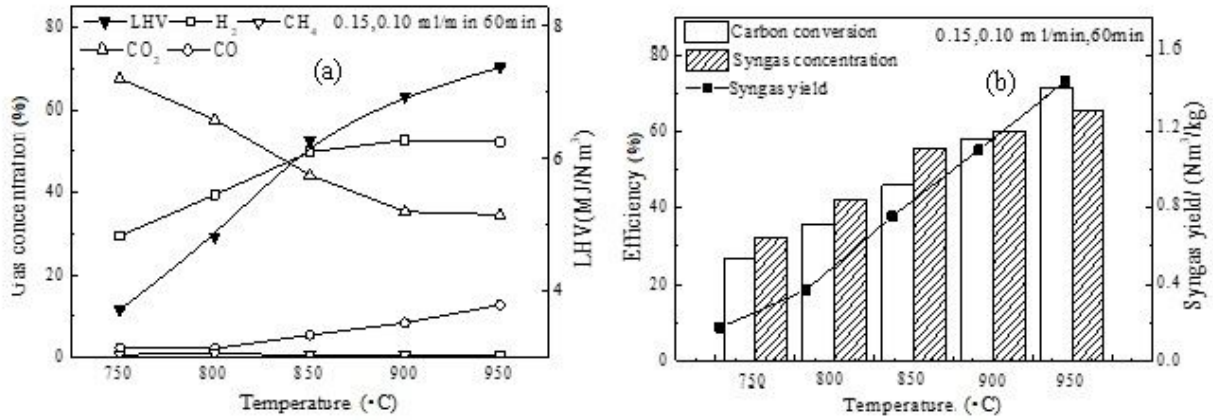

Figure 5

Gasification characteristics of WAC under different temperature

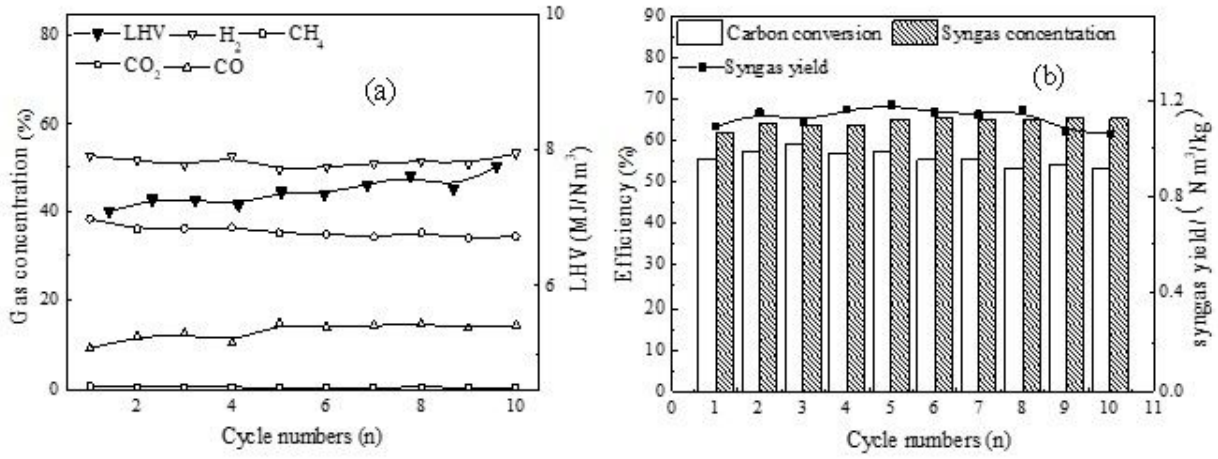

Figure 6

Gasification characteristics of WAC under different temperature

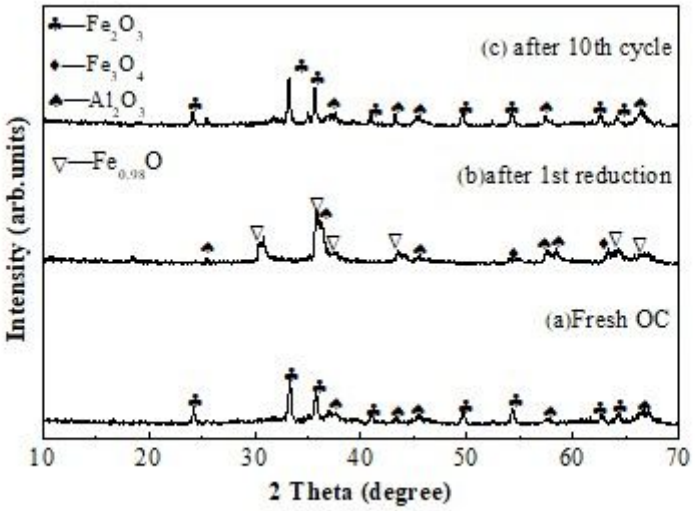

Figure 7

7XRD patterns of fresh and used OC samples

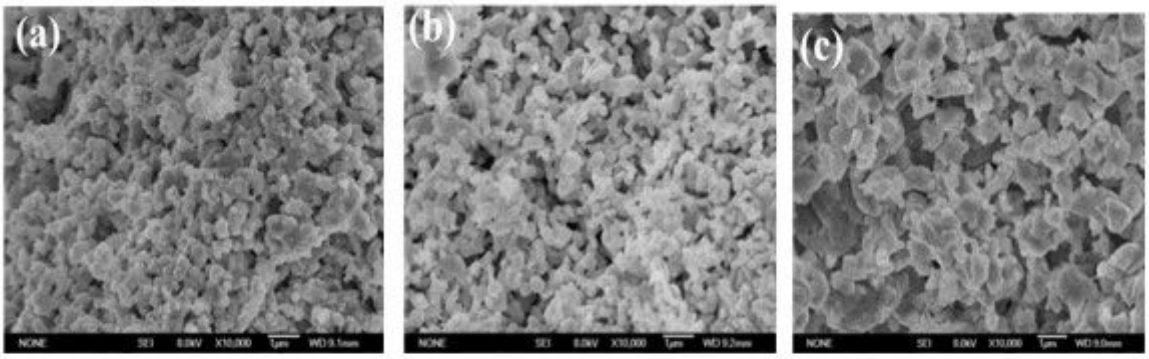

(a) Fresh sample (b) 1st sample (c) 10th sample

Figure 8

SEM images of Fresh and used OC samples